Rare Metal Materials and Engineering
Volume 51, Issue 5, May 2022
Available online at www.rmme.ac.cn

Science Press

Cite this article as: Lu Pengjian, Guan Jianguo, Zhang Song. Single-Crystalline Silver Nanobowls Synthesized by Self-Template Method[J]. Rare Metal Materials and Engineering, 2022, 51(05): 1597-1600.

ARTICLE

Single-Crystalline Silver Nanobowls Synthesized by Self-Template Method

Lu Pengjian, Guan Jianguo, Zhang Song

State Key Laboratory of Advanced Technology for Materials Synthesis and Processing, Wuhan University of Technology, Wuhan 430070, China

Abstract: The silver nanobowls were prepared by self-template method, and the structure and growth mechanism of Ag nanobowls were investigated. Results show that the Ag_2O clusters result from the reaction of $AgNO_3$ and NaOH. After adding the reductant methanal, Ag nano-shell is obtained on the Ag_2O cluster surface with the by-product CO_2 inside the Ag nano-shell. With the reaction further proceeding, the increasing pressure breaks through the Ag nano-shell, thereby forming the Ag nanobowls with the size of approximately 200 nm. This unique synthesis method provides theoretical and experiment basis for the noble metal nanomaterials with special structure.

Key words: noble metal; nanostructure; self-template

Metal nanomaterials have a special microstructure with a series of quantum size effects and are widely used in the chemical catalysis[1], antibacterial sterilization[2], optoelectronic devices[3], biological detection[4], and information storage[5] fields. In the atmospheric environment, the noble metal nanomaterials have higher stability and better electrical and catalytic properties than non-precious metals do[6]. Among the noble metals, the low-cost silver nanomaterials are widely used in electrical, optical, catalytic, and biomedical applications[7]. The resistivity of silver at room temperature is genuinely small of about 14.7×10^{-9} Ω·m. The silver nanomaterials exhibit strong ultraviolet (UV) -visible light absorption capacity due to their surface plasmons[8], and can promote the separation of photogenerated excitons and catalytic efficiency[9]. Besides, the silver nanomaterials have a strong antibacterial effect[10].

Compared with the nanocube, nanoflake, and nanobelt, nanobowls have larger surface area to volume ratio and higher surface activity[11]. However, due to the high oxidation degree and oxidation tendency of the non-precious metals, the oxide layer enlarges the point contact resistance between the particles, which deteriorates the optical, electrical, and catalytic properties of the silver nanoparticles[12]. At present, the silver nanomaterials are mainly prepared by the direct reduction method[13]. Based on different reaction principles, the direct reduction method can be divided into the light-induced reduction method[14], solvothermal reduction method, template reduction method[15], and microwave reduction method[16]. The template method can effectively control the morphology, structure, and size of silver nanomaterials, and is suitable for mass production. However, the templates used in the production are usually expensive and cannot be reused, which seriously restricts its application. The self-template method[17] has the advantages of both the template method and the solvothermal reduction method, such as simple synthesis steps, high reproducibility, low production cost, and controllable structure, because it uses the reaction intermediate product as the template.

In this research, the synthesis of single-crystalline silver nanobowls via the self-template method was proposed. The $AgNO_3$ was used as precursor to obtain Ag_2O clusters. Ag nanobowls were formed with the Ag_2O clusters as the templates. The material structure and growth mechanism were investigated.

1 Experiment

The silver nitrate ($AgNO_3$, AR, Aladdin), poly (N-vinyl-2-

Received date: May 21, 2021
Foundation item: Science Challenge Project (TZ2016001)
Corresponding author: Zhang Song, Ph. D., Professor, State Key Laboratory of Advanced Technology for Materials Synthesis and Processing, Wuhan University of Technology, Wuhan 430070, P. R. China, E-mail: kobe@whut.edu.cn

pyrrolidone) (PVP, MW40000, AR, Aladdin), sodium hydroxide (NaOH, AR, Aladdin), formaldehyde (CH_2O, AR, Aladdin), deionized water (10 MΩ·cm) were used in the this research.

After adding 40 mL $AgNO_3$ solution (0.001 mol/L) and PVP (m_{PVP}:m_{AgNO_3}=3:1), the 0.15 mol/L NaOH solution of 1 mL was added while the solution was vigorously stirred with a magnetic bar. After stirring for 20 min, 20 mL CH_2O solution (10vol%) was added. The reaction was conducted at 0 °C. The Ag nanobowls were separated by repeated centrifugations, washed by deionized water and ethanol, and finally redispersed into the deionized water.

The morphology of the as-prepared specimens was observed by a Hitachi S-4800 field-emission scanning electron microscope (SEM) at an acceleration voltage of 10.0 kV. The phase analyses of specimens were performed by X-ray diffraction (XRD) through the D/MAX-RB diffractometer using Cu Kα radiation with 2θ from 20° to 80°. The element composition of the specimens was characterized by a Horiba EX-250 X-ray energy dispersive spectrometer (EDS) operated at 20.0 kV coupled with SEM. The transmission electron microscopy (TEM) and the high-resolution transmission electron microscopy (HRTEM) were used through the H-600 STEM instrument at an acceleration voltage of 150 kV.

2 Results and Discussion

2.1 Morphology and structural analysis

SEM morphology of Ag nanobowls after CH_2O addition is shown in Fig. 1a. The diameter of Ag nanobowls is 60~200 nm. The orifice orientation of the nanobowls is random with the orifice size of 20~120 nm. The EDS spectrum demonstrates that the pure silver products are obtained (Fig. 1b). The typical face-centered cubic (fcc) structure of Ag (PDF 04-0783) is also revealed by XRD pattern (Fig. 1c). Four distinct diffraction peaks are observed at 2θ=38.1°, 44.3°, 64.4°, and 77.3°, corresponding to the (111), (200), (220), and (311) planes, respectively.

TEM images of Ag nanobowls are shown in Fig. 2. The thickness of the Ag nanobowl is about 20 nm and the inner diameter is about 120 nm. HRTEM image (Fig. 2c) and the selected area electron diffraction (SAED) pattern (inset of Fig. 2c) demonstrate that the Ag nanobowls are single-crystalline. The uniform lattice fringe spacing indicates the high-quality nanocrystal. The distance between each fringe is about 0.24 nm, corresponding to the interplanar distance of (111) planes.

2.2 Growth mechanism

The artificial polymer PVP is chemically inert. Fig. 3 shows the morphology of Ag nanobowls without PVP addition. It can be seen that some of the Ag nanobowls are cracked, which indicates that PVP serves as a surface stabilizer and nanoparticle dispersant. SEM images of Ag_2O nanoparticles before and after CH_2O addition are shown in Fig. 4. Fig. 4a shows the morphology of Ag_2O clusters after NaOH reacts with $AgNO_3$ solution. The Ag_2O clusters are formed by aggregation of Ag_2O nanoparticles with the diameter of 20 nm. The diameter of Ag_2O clusters is 80~150 nm, which is in accordance with the diameter of Ag nanobowls. It is inferred

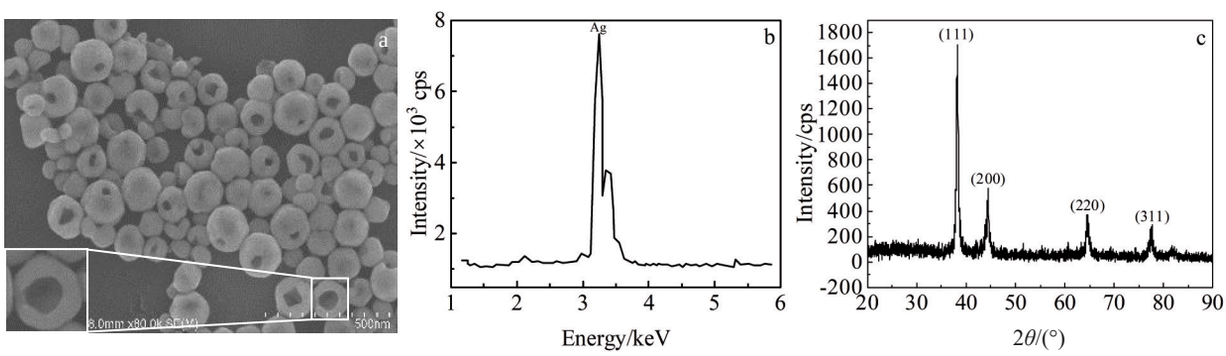

Fig.1 SEM morphology (a), EDS spectrum (b), and XRD pattern (c) of Ag nanobowls

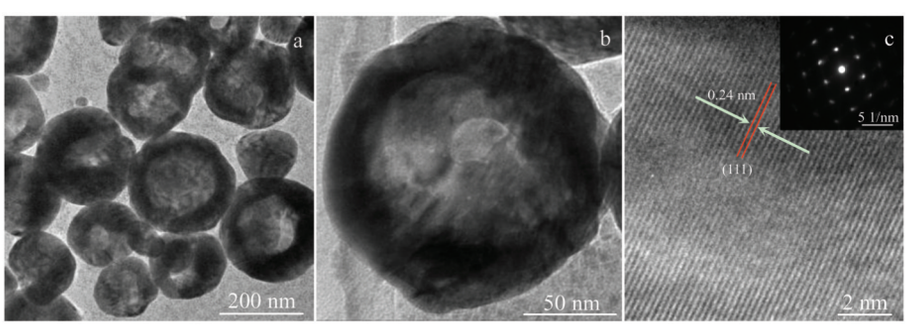

Fig.2 TEM images of Ag nanobowls (a, b); HRTEM image and SAED pattern of the shell of Ag nanobowls (c)

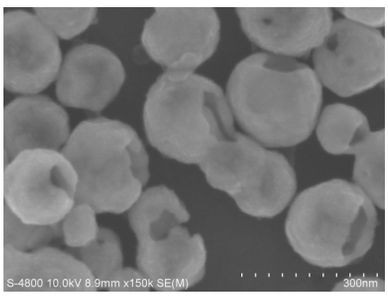

Fig.3 SEM morphology of Ag nanobowls without PVP addition

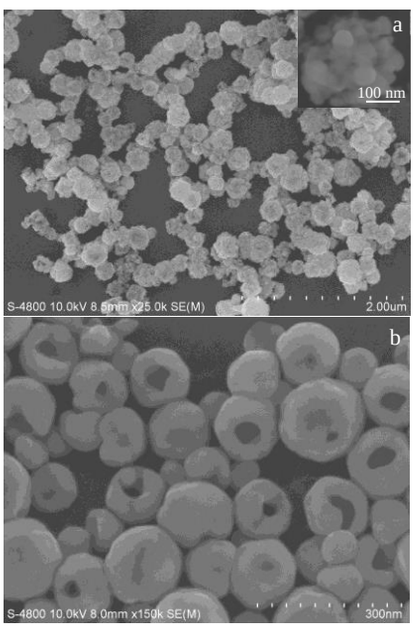

Fig.4 SEM morphologies of Ag_2O nanoparticles before (a) and after (b) CH_2O addition

that the Ag atoms are firstly formed on the Ag_2O cluster surface as a template. Then the CH_2O is diffused to the template surface and reduces the Ag_2O clusters. Some pinholes are covered by Ag atoms as the reaction proceeds. In addition, CO_2 bubbles are generated through the reduction. The involved chemical reactions are as follows:

$$2Ag^+ (l)+2OH^- (l) \rightarrow Ag_2O (s)+H_2O (l) \quad (1)$$

$$2Ag_2O (s)+CH_2O (l) \rightarrow 4Ag (s)+CO_2 (g)+H_2O (l) \quad (2)$$

As the reaction starts, CO_2 bubbles are released through the pinholes. With the reaction further proceeding, some pinholes are covered, and only one pinhole remains as the main channel and is enlarged by CO_2 bubbles, resulting in the bowl-like morphology.

In order to verify the necessity of gas bubbles during the growth of Ag nanobowls, $NaBH_4$ and $C_6H_8O_6$ are also used as the reductant. The related chemical reactions are as follows:

$$NaBH_4+4Ag^++4NaOH=4Ag+NaB(OH)_4+2H_2 (g)+4Na^+ \quad (3)$$

$$C_6H_8O_6+2Ag^+=C_6H_6O_6+2H^++2Ag \quad (4)$$

When $NaBH_4$ is used as the reductant (Fig. 5b), H_2 bubbles are generated. The Ag atoms firstly form on the Ag_2O particle

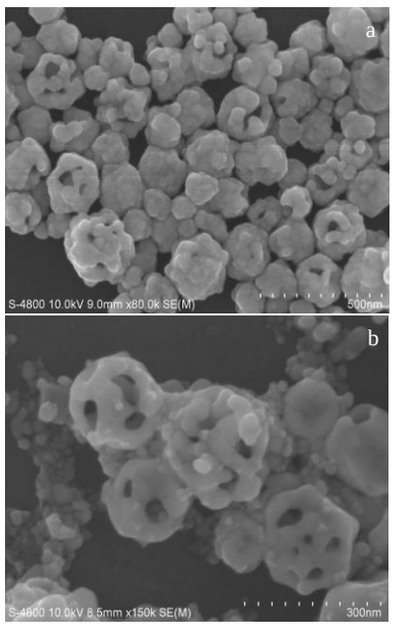

Fig.5 SEM morphologies of Ag nanobowls produced by reductant $C_6H_8O_6$ (a) and $NaBH_4$ (b)

surface and some pinholes are generated. Then, H_2 bubbles are released through the pinholes, resulting in the growth of multiple pores. Several pores on the surface are cage-like, which is different from the reduction product by CH_2O. The strong reducibility of $NaBH_4$ promotes the releasing rate of H_2 bubbles, resulting in the enlargement of several pinholes. The reaction rate of CH_2O is relatively slow, compared with that of $NaBH_4$ reductant, and therefore CO_2 gas is accumulated slowly inside the clusters and covered by Ag nano-shell. When CO_2 gas accumulates to a certain amount, a big hole is formed to release the increasing pressure inside the Ag nano-shell. When $C_6H_8O_6$ is used as the reductant, no gas is produced during the whole reaction, and therefore some irregular pinholes appear on the cluster surface due to the incomplete deposition of Ag atoms.

Thus, the growth mechanism of Ag nanobowls is shown in Fig. 6: (I) the formation of Ag_2O nano-crystallites; (II) the spherical aggregation of Ag_2O clusters; (III) the reduction of

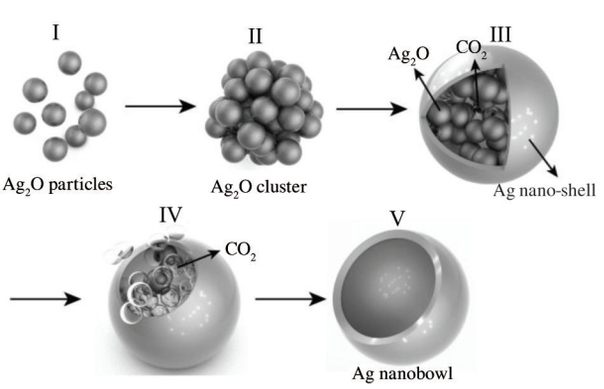

Fig.6 Schematic diagram of growth mechanism of Ag nanobowls

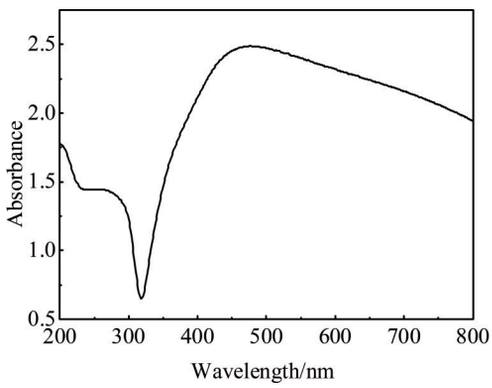

Fig.7 UV-visible spectrum of Ag nanobowls

Ag_2O to Ag; (IV) the formation of hollow structures; (V) the growth of main pore on the surface caused by the release of CO_2 gas and the formation of bowl-like morphology.

The position of the plasmon absorption peak depends on the particle size and shape. The UV-visible spectra of the silver nanobowls is shown in Fig. 7. The Ag nanoparticles display the plasmon absorption in the visible region and usually have the maximum absorption at 404 nm, while Ag nanobowls display the maximum absorption at 478 nm, which is red-shifted about 73 nm, indicating a good optical property. The resonance features are quite broad due to the diversity of nanobowl dimensions.

3 Conclusions

1) The Ag nanobowls can be synthesized by self-template method at low temperature.

2) The formation mechanism contains five steps: (I) the formation of Ag_2O nano-crystallites; (II) the spherical aggregation of Ag_2O clusters; (III) the reduction of Ag_2O to Ag; (IV) the formation of hollow structures; (V) the growth of main pore on the surface caused by the release of CO_2 gas and the formation of bowl-like morphology. The release of CO_2 bubbles inside the Ag nano-shell plays an important part in the formation of bowl-like structures.

3) The Ag nanobowls have good optical properties and can be applied in biomedical, biomolecular detection, and catalysis fields. This research provides a theoretical and experiment basis for the preparation of hollow and porous nanostructures of different metals.

References

1 Huang Hehan, Xia Li, Shi Xifeng *et al*. *Chemical Communications*[J], 2018, 54(81): 11 427
2 Zhou Liang, Liu Zhihang, Guan Zhipeng *et al*. *Applied Catalysis B: Environmental*[J], 2020, 263: 118 326
3 Kim Jinwook, Ouyang Dan, Lu Haifei *et al*. *Advanced Energy Materials*[J], 2020, 10(15): 1 903 919
4 Murphy C J, Vartanian A M, Geiger F M *et al*. *ACS Central Science*[J], 2015, 1(3): 117
5 Jiang H, Belkin D, Savel'ev S E *et al*. *Nature Communications* [J], 2017, 8(1): 1
6 Hamid Heidarzadeh. *Optics Communications*[J], 2020, 459: 124 940
7 Mallon C T, Kho K W, Gartite H *et al*. *Advanced Engineering Materials*[J], 2018, 20(1): 1 700 532
8 Zhang Linlin, Sha Jianang, Chen Rongrong *et al*. *Applied Catalysis B: Environmental*[J], 2020, 271: 118 920
9 Johnson A D, Cheng F, Tsai Y *et al*. *Nano Letters*[J], 2017, 17(7): 4317
10 Ran Xiang, Du Ye, Wang Zhenzhen *et al*. *ACS Applied Materials and Interfaces*[J], 2017, 9(23): 19 717
11 Yan Zihao, Taylor M G, Mascareno A *et al*. *Nano Letters*[J], 2018, 18(4): 2696
12 Yang T H, Shi Y, Janssen A *et al*. *Angewandte Chemie International Edition*[J], 2020, 59(36): 15 378
13 Fu Liangjie, Yan Zhaoli, Zhao Qihang *et al*. *Advanced Materials Interfaces*[J], 2018, 5(23): 1 801 094
14 Cui Can, Wang Yaping, Liang Dayu *et al*. *Applied Catalysis B: Environmental*[J], 2014, 158-159: 150
15 Liu Yanjun, Xu Chunxiang, Lu Junfeng *et al*. *Applied Surface Science*[J], 2018, 427(A): 830
16 Liu Sen, Tian Jingqi, Wang Lei *et al*. *Journal of Nanoparticle Research*[J], 2011, 13(10): 4539
17 Zhang Yehui, Li Jiajing, Rong Heng *et al*. *Langmuir*[J], 2017, 33(24): 5991

自模板法合成银纳米碗

卢鹏荐，官建国，章　嵩
(武汉理工大学 材料复合新技术国家重点实验室，湖北 武汉 430070)

摘　要：采用自模板法合成了碗状银纳米材料，研究了银纳米碗的结构和生长机理。结果表明：$AgNO_3$和NaOH反应生成Ag_2O纳米簇，然后加入还原剂甲醛，在Ag_2O模板表面形成Ag纳米壳，副产物CO_2则在Ag壳内聚集。随着反应的进行，不断增大的压力最终击穿Ag壳，形成了直径约为200 nm的Ag纳米碗。该方法为特殊结构贵金属纳米材料的研究提供了理论和实验基础。

关键词：贵金属；纳米结构；自模板法

作者简介：卢鹏荐，男，1984年生，博士生，武汉理工大学材料复合新技术国家重点实验室，湖北 武汉 430070，E-mail：109969814@qq.com